Civil Engineering Infrastructures Journal xx,xx

DOI: 10.22059/ceij.2026.400057.2361

Technical Notes

# Numerical Analysis of PVC and HDPE Pipe Deformation under EPS-Derived Aggregates



Rakesh Kumar Dutta[1], Tammineni Gnananandarao[2*], Sourabh Kumar[1], Vishwas Nandkishor Khatri[3], V. Gayathri[4]

[1]Department of Civil Engineering, National Institute of Technology, Hamirpur, Himachal Pradesh, India, 177005. rkd@nith.ac.in

sourabhdogra90@gmail.com

[2*]Department of Civil Engineering, Aditya University, Surampalem, India, 533437. anandrcwing@gmail.com

[3]Department of Civil Engineering, Indian Institute of Technology (Indian School of Mines), Dhanbad, Jharkhand, 826004, India vishuiisc@gmail.com

[4]Department of Civil Engineering, Kumaraguru College of Technology, Coimbatore 641049, Tamil Nadu, India;

gayathri.v.ce@kct.ac.in

[*]Corresponding author: anandrcwing@gmail.com ORCID iD: 0000-0002-3332-8083

Received: 17/09/2025

Revised: 17/02/2026

Accepted: 28/04/2026

## Abstract

This research aims to study the deformation behavior of polyvinyl chloride (PVC) and high-density polyethylene (HDPE) pipe buried in the trench containing various types of materials such as sand, sand-EPS (Expanded Polystyrene) derived aggregate, and sand-fly ash-cement-EPS derived aggregate. The sizes of beads in the range of 4-5 mm were considered for modelling, and EPS content varied from 0.05 to 0.20% for the sand-EPS derived aggregates and 0.25 to 0.45% for the sand-fly ash-cement-EPS derived aggregates. Other variables such as pipe diameter (from 0.5 to 1.2 m) and placing depth (from 0.3 to 0.9 m) were also considered.

Results show that PVC and HDPE pipes generally have reduced deformations when wrapped with sand-EPS derived aggregate, with the exception of larger pipes with increased deformations at the bottom and left side of the pipe. On the other hand, sand-fly ash-cement-EPS derived aggregate, the deformation decreases with PVC pipes (0.5 m diameter) but increases in the case of larger HDPE pipes (0.9 m diameter) at several points. The deformation patterns of sand-EPS derived aggregates vary with the pipe diameter when the fill depth changes, smaller pipe diameter (0.5 m) has less deformation, while larger pipe diameter (0.9 m) has the opposite trend. The deformation decreases at all points for the HDPE pipes (0.9 m diameter), while for the larger diameter pipes (1.2 m), the deformation trend changes at certain points. The results of this study may help to understand the use of compressible material as a backfill for underground pipes and the different behaviours of the pipes when exposed to these materials depending on pipe material, pipe diameter and backfill material.

**Keywords:** PVC, HDPE, Finite element analysis, EPS-sand mixture, EPS-fly ash.

## 1. INTRODUCTION

Expanded polystyrene (EPS) geofoam has become significantly popular since its first application as thermal insulation for pavements in the 1960s (Horvath, 2003). Following its introduction as a lightweight fill material by the Norwegian Road Research Laboratory (NRRL) in the early 1970s, EPS usage expanded rapidly on a global scale (Hazarika, 2006; Lee et al., 2003; Tammineni Gnananandarao, Rakesh Kumar Dutta, 2022). Using EPS as a lightweight fill material is especially beneficial when reducing earth loads is required due to weak subsoil conditions (Bartlett, 2000). As a result, research on EPS as a geoengineering material has increased alongside its broader utilization in the geotechnical field. Since the late 1980s, EPS's role as a compressible inclusion has emerged and found widespread practical application. (A . M. Partos and P . M. Kazaniwsky, 1987; Horvath, 1998; Khajeh et al., 2020; J. Vaslestad et al., n.d.; Zhu et al., 2022) suggested to utilizing EPS as a compressible inclusion around a buried pipe to lighten the vertical earth load on the pipe. They advised a minimum thickness of 500 mm and a minimum width exceeding 1.5 times the pipe diameter, based on findings from three field case studies. (Kumar et al., 2025; J. , J. T. H. , and H. W. , Vaslestad, 1994). EPS serves as a feasible substitute for organic materials as a compressible inclusion around pipes. Its dependable performance has been well-documented for over 40 years. Moreover, its mechanical properties, including strength, can be conveniently regulated in a factory by adjusting its density (Bartlett, 2000). Despite being proposed as a material for compressible inclusion, there is limited literature providing recommendations on the ideal geometry for such inclusion in induced trench systems. Even the few available recommendations lack quantitative consistency. According to (Kim and Yoo, 2005) analytical study, the optimal geometry of compressible inclusions needs further refinement due to insignificant load reduction achieved when the width surpasses 1.5 times the pipe diameter. Moreover, incorporating multiple layers of compressible inclusions may aid in decreasing earth pressure on buried pipes. This concept began with (Spangler, n.d.), who stacked layers of leaves and loose soil to mimic a trench above buried pipe. In situations where a buried pipe is installed beneath high embankments or in less-than-ideal trench conditions, a plane of uniform settlement forms within the embankment. (Spangler, 1950)found that this plane is located approximately 1.12 m above the pipe's top when the embankment is present. Placing a compressible inclusion above this plane can induce relative settlement between the soil prism and adjacent soils, mobilizing shear strength and reducing overburden pressure. Now a days, engineers use EPS geofoam blocks for the same purpose (Khalaj, Azizian, et al., 2020; Khan and Meguid, 2021; Kliszczewicz and Kowalska, 2020; Onyelowe et al., 2022). When EPS geofoam is placed over a rigid pipe, it compresses more than the surrounding fill. This mismatch forces the stiffer soil on either side to span across the soft zone and form an arch over the pipe. As a result, most of the vertical load is carried laterally by the soil arch, reducing pressure on the pipe crown and increasing tension along its side walls. The soft EPS layer also let's shear stresses develop exactly where this arching occurs, further strengthening the effect. Multiple studies have confirmed that using EPS geofoam in this "imperfect trench" setup cuts pipe deflection significantly (Abdollahi et al., 2021; Azizian et al., 2020; Khalaj, Siabil, et al., 2020; Onyelowe et al., 2021; J. Vaslestad et al., n.d.). Numerical analyses have also explored the soil–structure interaction in these installations, showing consistent load redistribution benefits(Chen et al., 2020; Kang et al., 2020; Santos et al., 2020; J. Vaslestad et al., n.d.) .

However, no numerical study has explored till date the deformation behaviour of PVC/HDPE pipes buried inside the sand, sand-EPS derived aggregate and sand-fly ash-cement-EPS derived aggregate. To fill this gap in literature, the current study was conducted to understand the deformation behaviour of PVC/HDPE pipes buried inside the sand, sand-EPS derived aggregate and sand-fly ash-cement-EPS derived aggregate. This objective was achieved through the execution of a series of numerical investigations. The factors considered in the numerical investigations comprised of the diameter of pipes and the depth of fill material.

## 2. PROBLEM DEFINITION, PARAMETERS VARIED AND MESH CONVERGENCE STUDY

A numerical investigation was conducted on PVC and HDPE pipes of varying diameters buried in trenches filled with composite backfill materials comprising sand, sand-EPS-derived aggregate, and sand-fly ash-cement-EPS-derived aggregate. Figures 1 and 2 illustrate the problem definition. The numerical model measured 12 m × 12 m × 6 m (length × width × depth). Pipe diameters ranged from 0.5 to 1.2 m, while burial depths varied between 0.3 and 0.9 m. The trench was embedded in soft clay and backfilled with the selected composite materials. The parameters considered in the analysis and the engineering properties of the backfill materials are summarized in Table 1 and Tables 2–3, respectively. Figure 1 presents the longitudinal sectional view showing the pipe location and composite backfill within the surrounding soft clay, whereas Figure 5 illustrates the plan view of the finite element mesh with refined elements near the trench and progressively coarser elements away from the pipe.

Table 1 Summary of parameter varied

| Parametric study | Size of EPS beads (mm) | Fly ash (%) | Cement (%) | EPS Beads (%) | Diameter of PVC and HDPE pipes (m) | Placement depth of PVC/HDPE in trench (m) |
|---|---|---|---|---|---|---|
| Effect of EPS content | 4-5 | | | 0, 0.05, 0.12, 0.20 | 0.5, 0.9, 1.2 | 0.3, 0.6, 0.9 |
| Effect of fly ash content | 4-5 | 0, 6, 12 | 4 | 0.25, 0.35, 0.45 | 0.5, 0.9, 1.2 | 0.3, 0.6, 0.9 |
| Ratio of diameter to placement depth of pipe (Dp/DT) | 4-5 | ------ | ------ | 0.2 | 0.5, 0.9, 1.2 | 0.3, 0.6, 0.9 |

Table 2 Properties of various mixes of sand-EPS beads for modelling

| Combinations | EPS content (%) | Cohesion (c, kPa) | Friction angle (ϕ) | Modulus (E, MPa) | Poisson ratio (ν) |
|---|---|---|---|---|---|
| Sand + EPS beads (4-5 mm ) (after (Yaghoobzadeh et al., 2021) | 0.0509 | 5.7 | 22.6 | 6.78 | 0.25 |
| | 0.1145 | 6.9 | 20.4 | 6.04 | 0.2 |
| | 0.1962 | 11.8 | 18.1 | 4.2 | 0.25 |
| Clay Properties ( after (Talal Awwad; Salma Al Kodsi, 2018) | ------ | 13.5 | 5 | 7500 | 0.45 |
| Sand-EPS beads and fly ash properties (After (Khajeh et al., 2020) | 0.25 | 112 | 30 | 7.44 | 0.25 |
| | 0.35 | 101.33 | 26.5 | 6.45 | 0.24 |
| | 0.45 | 95.33 | 23 | 4.17 | 0.23 |

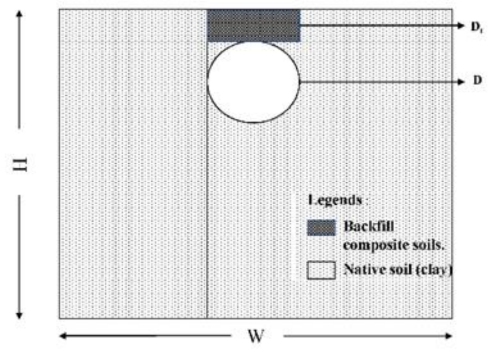


**Figure.1** Problem statement

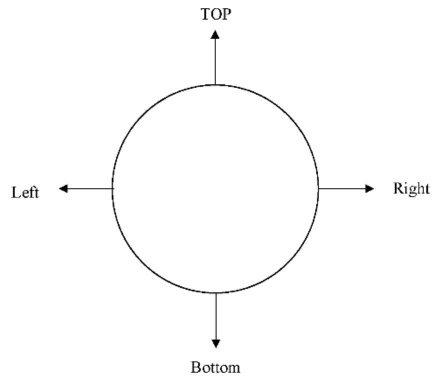


**Figure.2** Pipe layout

Table 3 Properties of PVC/HDPE pipe used for modelling

| Material of pipe | Pipe diameter(m) | Density ($kN/m^2$) | Young's Modulus (E, MPa) | Poisson Ratio (v) |
|---|---|---|---|---|
| PVC (after (A. Kuliczkowski, 2001) | 0.5 | 14.0 | 3200 | 0.24 |
| PVC (After(Chaallal et al., 2014)) | 0.9 | 13.8 | 2760 | 0.37 |
| HDPE (After (Chaallal et al., 2014)) | 0.9 | 9.3 | 760 | 0.4 |
| HDPE (After (Chaallal et al., 2014) ) | 1.2 | 9.7 | 760 | 0.4 |

The properties shown in Table 2 and Table 3 were taken from literature (Chaallal et al., 2014; Khajeh et al., 2020; Talal Awwad; Salma Al Kodsi, 2018; Yaghoobzadeh et al., 2021). The entire methodology is depicted in the flow chat and shown in Fig. 3.

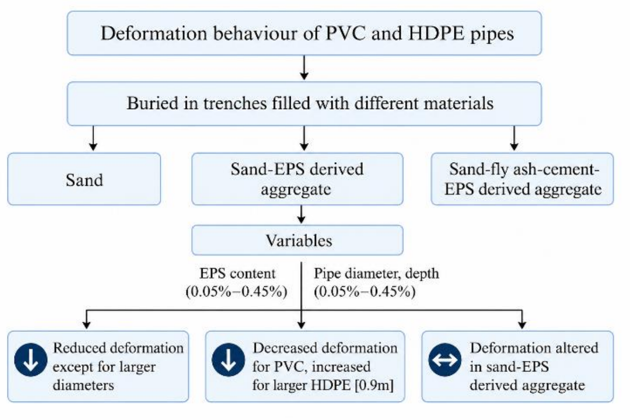


Fig. 3 Methodological flowchart

The deformation behaviour of PVC and HDPE pipes embedded in sand, sand-EPS-derived aggregate, and sand-fly ash-cement-EPS-derived aggregate was investigated using finite element analysis in ABAQUS, based on the model shown in Figure 1. Pipe deformation was measured at the centre of the applied loading area by monitoring the corresponding nodal displacement. The PVC and HDPE pipes were modelled as linear elastic materials, whereas the backfill materials were represented using the elastic-perfectly plastic Mohr–Coulomb constitutive model. Material properties adopted in the analysis are summarized in Tables 1–3.

The pipe–soil interaction was simulated using a surface-to-surface contact formulation. A hard contact model was assigned in the normal direction, while tangential behaviour was represented using a penalty friction model. The interface friction coefficient (μ) was calculated using Eq. (1):

$$\mu = \tan(\delta) \qquad (1)$$

where δ is the interface friction angle. Following literature recommendations, δ was assumed as 0.67ϕ for sand-based materials, providing realistic slip and stress transfer between the pipe and surrounding soil.

An eight-node linear brick element with reduced integration (C3D8R) was used for modelling the composite backfill materials. The surrounding soft clay was simulated as normally consolidated clay, emphasizing undrained shear strength characteristics as recommended by (Schmidt, 2011). The coefficient of earth pressure at rest was taken as $K_0 = 0.95$, consistent with (Castro, 2017). The numerical model dimensions (12 m × 12 m × 6 m) were selected to minimize boundary effects by maintaining lateral boundaries at least five times the maximum pipe diameter from the pipe centreline. As shown in Figure 4, the bottom boundary was fixed, while the side boundaries were restrained horizontally and allowed vertical movement. Initial in-situ stresses were established using a geostatic step with gravity loading, followed by trench excavation, composite backfilling, and loading, ensuring realistic simulation of soil–pipe interaction.

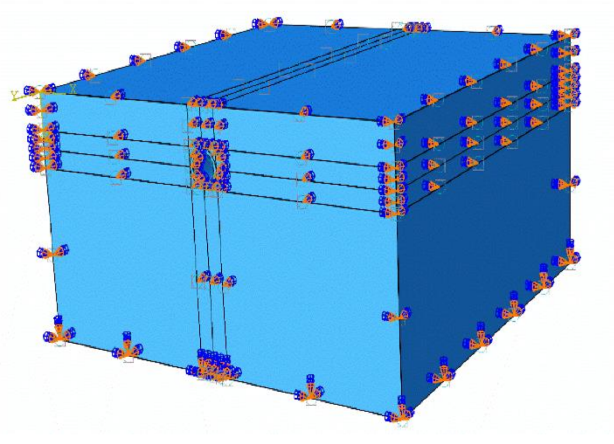

Figure.4 Boundary condition

The interface friction between the soft clay and surrounding sand, sand-EPS derived aggregate and sand-fly ash-cement-EPS derived aggregate were calculated by the formula as suggested by (Shahu and Reddy, 2011). Figure 5 illustrates how the meshing became coarser as one moved away from the trench and became finer near it.

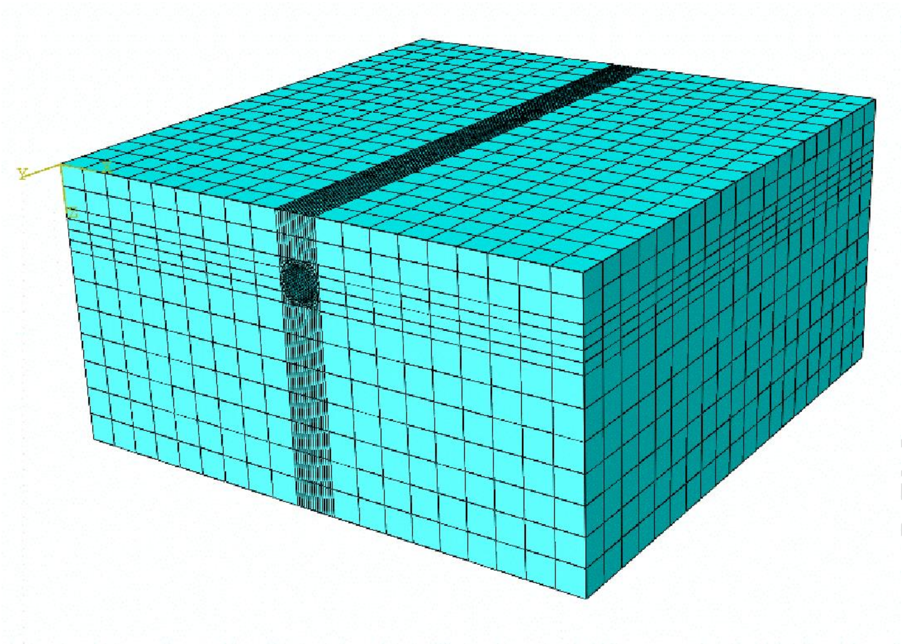

Figure.5 Meshing of the model

For elements greater than 33,180, mesh convergence study showed negligible effects on deformation at the pipe crucial points. Since additional mesh refinement did not significantly modify the deformation, which remained at 1.53 %, the subsequent numerical study picked 33,180 elements, as shown in Table 4.

Table 4 Mesh convergence study

| S. No. | Number of mesh elements | Maximum load (kN) | Percentage error |
|---|---|---|---|
| 1 | 28665 | 590.85 | - |
| 2 | 33180 | 256.82 | 13.60% |
| 3 | 33668 | 751.351 | 1.53% |

Although the geometry and loading are symmetric, a full 3D model was adopted instead of utilizing symmetry boundary conditions. This decision was made because nonlinear soil behaviour, contact interface friction, and staged construction can introduce localized plastic strain development and minor asymmetrical stress redistribution. Small differences in deformation observed on the left and right sides of the pipe result from material nonlinearity and contact mechanics rather than geometric asymmetry. Using a full model ensured that such realistic soil–structure interaction effects were properly captured.

## 3. SOFTWARE VALIDATION

Before conducting the parametric study, the numerical model was validated against the results reported by (Kliszczewicz and Kowalska, 2020). The validation employed the same material properties, including friction angle, dilatancy angle, unit weight, cohesion, and elastic modulus for native soil, backfill, and tire-derived aggregate (TDA). A Poisson's ratio of 0.25 was adopted based on (Edil and Bosscher, 1994). The finite element analysis was performed using the Mohr–Coulomb constitutive model. Boundary conditions allowed vertical movement along the side boundaries while restraining horizontal displacement, with the bottom boundary fully fixed. The validation results are presented in Figure 6.

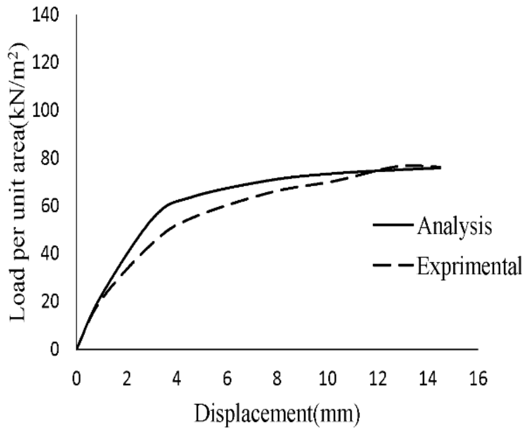


Figure.6 Comparison of result from experimental value and numerical model.

Study of Figure. 6 reveals that the vertical stress above PVC pipe crown and varying thickness of TDA agreed within 1.96 %. The minor difference in the results can be attributed to the difference in the properties of the materials used in the previous and the current study.

# 4. RESULTS

## 4.1 Influence of coarse EPS content on deformation of PVC and HDPE pipe

The influence of EPS content in the deformation of the PVC and HDPE pipes are presented in Figure 7 to Figure 10.

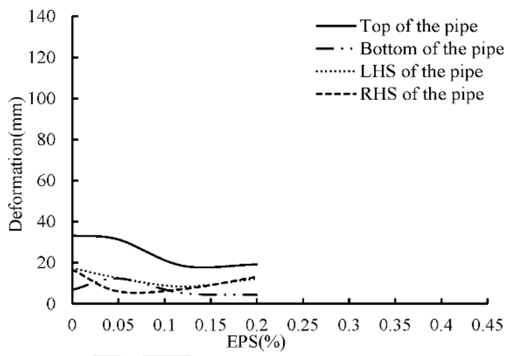


Figure. 7 Variation of deformation with EPS content deformation for sand and backfill in different combinations for 0.5-meter-diameter flexible PVC pipe positioned at a depth of 0.3 meters.

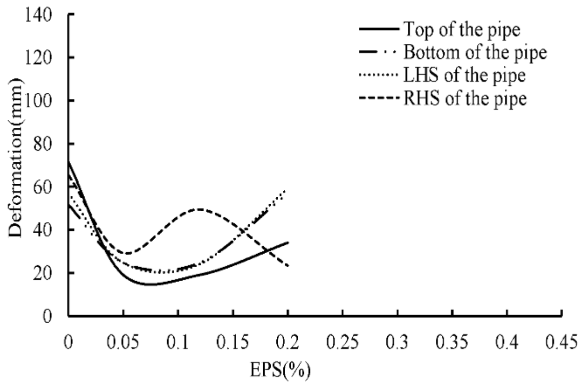


Figure. 8 Variation of deformation with EPS content deformation for sand and backfill in different combinations for 0.9-meter-diameter flexible PVC pipe positioned at a depth of 0.3 meters.

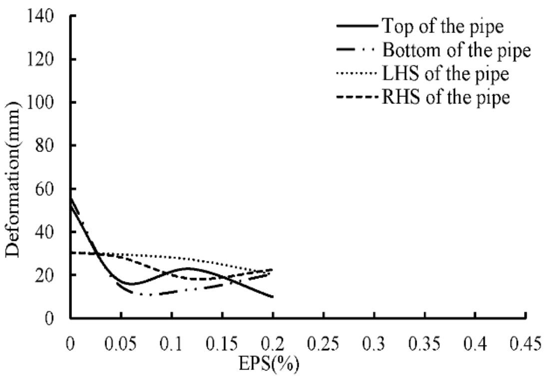


Figure.9 Variation of deformation with EPS content deformation for sand and backfill in different combinations for 0.9-meter-diameter flexible HDPE pipe positioned at a depth of 0.3 meters.

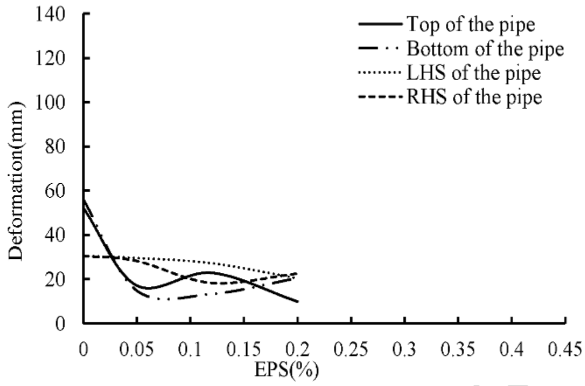


Figure.10 Variation of deformation with EPS content deformation for sand and backfill in different combinations for 1.2-meter-diameter flexible HDPE pipe positioned at a depth of 0.3 meters.

Figures 7 and 8 illustrate the effect of varying coarse EPS content on the deformation behaviour of PVC pipes. The results indicate a clear relationship between EPS content and pipe deformation. For the 0.5 m diameter PVC pipe (Figure 7), increasing EPS content significantly reduced deformation in the top (42.83%), bottom (36.34%), left (29.41%), and right (21.09%) sections. However, localized increases in deformation were observed at 0.20% EPS in the bottom region and 0.12% EPS on the left side, indicating the presence of stress concentrations. Similarly, Figure 8 shows that for the 0.9 m diameter PVC pipe, increasing EPS content substantially reduced deformation in the top (52.48%) and right (64.31%) sections. In contrast, comparatively smaller reductions were observed in the bottom (10.10%) and left (3.97%) regions, suggesting that certain stress components were not fully mitigated by EPS reinforcement. These observations demonstrate that although EPS-derived aggregates effectively reduce overall pipe deformation by improving backfill stiffness and load distribution, localized deformation may still occur due to complex soil–pipe interaction and stress redistribution.

The influence of EPS content on the deformation behaviour of HDPE pipes is presented in Figures 9 and 10. Similar to PVC pipes, increasing EPS content consistently reduced deformation in most regions. For the 0.9 m diameter HDPE pipe (Figure 9), deformation decreased markedly in the top (81.10%), bottom (63.40%), left (33.16%), and right (26.21%) sections with increasing EPS content. Likewise, Figure 10 shows that for the 1.2 m diameter HDPE pipe, higher EPS content reduced deformation in the top (23.57%) and right (6.36%) sections, while significant reductions were also observed at the bottom (36.68%) and left (24.13%) regions. The improved performance is primarily attributed to the lightweight and compressible nature of EPS-derived aggregates, which enhance backfill stiffness, promote soil arching, redistribute applied loads, and reduce vertical earth pressure acting on the pipes. Nevertheless, localized stress concentrations may still develop, resulting in non-uniform deformation patterns. Overall, the results presented in Figures 7–10 demonstrate that incorporating EPS-derived aggregates significantly improves the deformation performance of both PVC and HDPE pipes. The extent of improvement depends on pipe diameter, EPS content, and the interaction between the pipe and surrounding soil, emphasizing the importance of optimizing backfill composition for enhanced buried pipe performance.

### 4.2 Influence of adding fly ash in sand-EPS derived aggregate on deformation of PVC and HDPE pipe

The influence of fly ash in sand-EPS derived aggregates content in the deformation of the PVC and HDPE pipes are presented in Figure 11 to Figure 12.

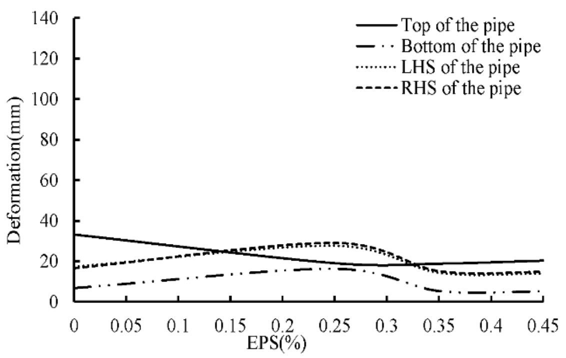


Figure. 11 Variation of deformation with EPS content deformation for sand and backfill in different combinations for 0.5-meter-diameter flexible PVC pipe positioned at a depth of 0.3 meters.

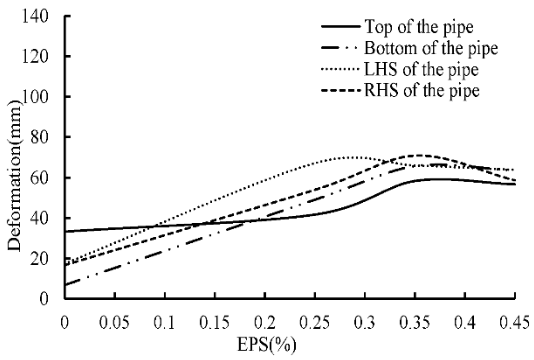


Figure. 12 Variation of deformation with EPS content deformation for sand and backfill in different combinations for 0.9-meter-diameter flexible PVC pipe positioned at a depth of 0.3 meters.

The deformation behaviour of flexible PVC pipes used in the composite sand–EPS derived aggregate and when fly ash is added to this composite is given in Figures 11 and 12, respectively. For 0.5 m diameter PVC pipe in Figure 11, the top, bottom, left and right side deformations showed a decrease of 38.82%, 24.10%, 19.69%, and 11.27% respectively because of the presence of fly ash. For the same PVC pipe with a diameter of 0.9 m, the effect of fly ash, according to Fig. 12, is different: in the upper part of the pipe (41.39%), its presence causes an increase in the deformation, in the lower part (89.33%) it causes an increase in the deformation, and in the left side part (72.80%) it causes an increase in the deformation, but in the right side part (71.67%) it causes a decrease in deformation. The results show that the effect of fly ash on pipe deformation can be a complex case and depends on the stress distribution and pipe diameter. Fly ash can enhance the structural performance in various instances but can also result in changes in the stress redistribution and deformation in localized areas. Relevant behaviour of flexible HDPE pipes is presented in Figures 13 and 14.

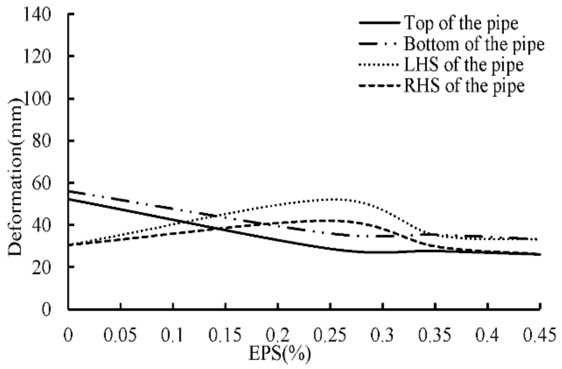


Figure. 13 Variation of deformation with EPS content deformation for sand and backfill in different combinations for 0.9-meter-diameter flexible HDPE pipe positioned at a depth of 0.3 meters.

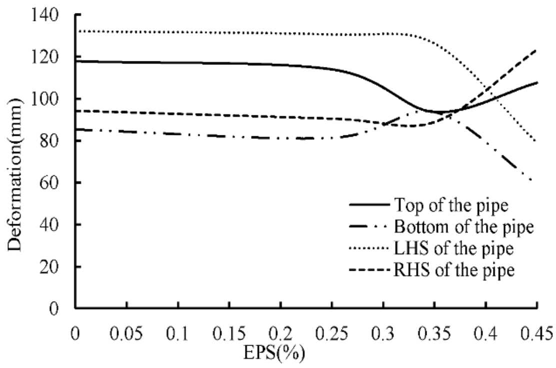


Figure. 14 Variation of deformation with EPS content deformation for sand and backfill in different combinations for 1.2-meter-diameter flexible HDPE pipe positioned at a depth of 0.3 meters.

To understand the effect of addition of fly ash in sand–EPS derived aggregate composite on the deformation behaviour of flexible HDPE pipes, the Figures 13 and 14 are provided here. For 0.9 m HDPE pipe (Figure 13), you can see that the deformation was found to be significantly reduced in the top (50.19%), bottom (40.71%) and right (14.28%) parts of the pipe. The opposite trend however was observed for the left part, showing a slight increase in deformation (8.53%), which can be interpreted as areas of local stress concentrations. The overall results indicate that use of fly ash would be beneficial for the deformation resistance of the composite backfill in most areas of the pipe by increasing the stiffness and load distribution performance of the composite backfill material.

For the 1.2 m diameter HDPE pipe (Figure 14) the same characteristics are evident. Deformation in the top, bottom and left sections decreased after the addition of the fly ash (8.49%, 30.60%, 40.27%) whereas deformation in the right section increased (30.89%). This signifies that the advantageous consequences of fly ash aren't constant along the pipe and might be dependent on the redistribution of the stress or inhomogeneity of the soil–pipe interaction.

Inflexibility of pipes depends on various parameters due to the influence of fly ash on the mechanical behaviour of flexible HDPE pipes as shown in Figures 13 and 14, respectively. Generally, the use of fly ash results in an increase in stiffness of the composite backfill, decrease in pipe movement and greater uniformity in load transfer, while maintaining structural performance. The large reductions in top and bottom sections show that performance of the modified backfill has been able to reduce vertical stresses and minimise pipe deflection. Despite overall uniformity of deformation, localized higher levels of deformation (e.g. left side of Figure 13 and right side of Figure 14) indicate potential stress concentrations arising from the non-uniform nature of the material behaviour and complex interaction of soils and structures. These changes suggest that pipe response will be influenced by factors such as pipe diameter, loading conditions, and the interaction between the pipe and the surrounding composite backfill, in addition to the presence of fly ash. In conclusion, fly ash can typically be used to enhance the deformation behaviors of flexible HDPE pipes, but further research is needed to determine the optimal amount of fly ash needed to be incorporated into the sand–EPS composite aggregate and the stress redistribution mechanisms involved to enable superior long-term pipe performance.

### 4.3 Influence of depth of coarse EPS backfill on deformation of PVC and HDPE pipe.

The influence of fly ash in sand-EPS derived aggregates content in the deformation of the PVC and HDPE pipes are presented in Figure 15 to Figure 18.

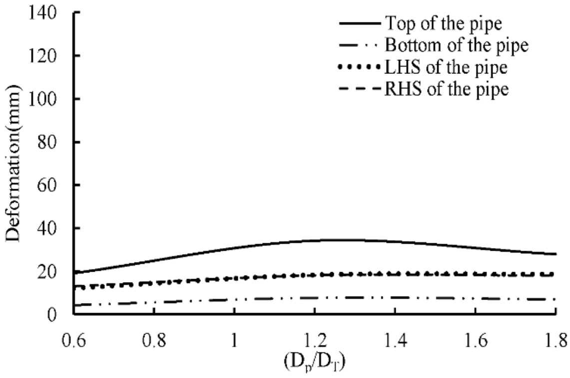


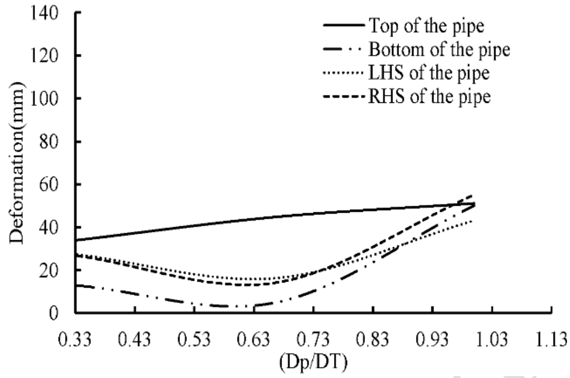


Figure. 15 Variation of deformation with $D_p/D_t$ content deformation for sand and backfill in different combinations for 0.5-meter-diameter flexible PVC pipe positioned at a depth of 0.3,0.6,0.9 meters.

Figure. 16 Variation of deformation with $D_p/D_t$ content deformation for sand and backfill in different combinations for 0.9-meter-diameter flexible PVC pipe positioned at a depth of 0.3,0.6,0.9 meters

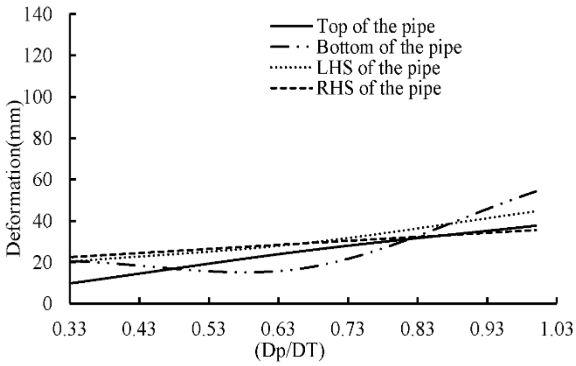


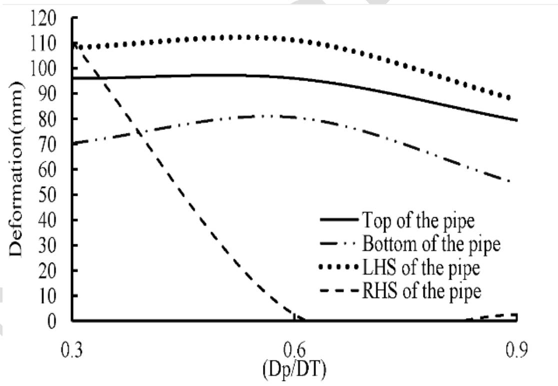


Figure. 17 Variation of deformation with $D_p/D_t$ content deformation for sand and backfill in different combinations for 0.9-meter-diameter flexible HDPE pipe positioned at a depth of 0.3,0.6,0.9 meters

Figure.18 Variation of deformation with $D_p/D_t$ content deformation for sand and backfill in different combinations for 1.2-meter-diameter flexible HDPE pipe positioned at a depth of 0.3,0.6,0.9 meters

Figures 15 and 16 illustrate the influence of backfill depth on the deformation behaviour of flexible PVC pipes containing EPS-based composite backfill. As the backfill depth above the pipe increases, deformation generally increases due to the higher vertical earth pressure. In Figure 15, for the 0.5 m diameter PVC pipe, increased backfill depth resulted in noticeable deformation in the top, bottom, left, and right sections. Similarly, Figure 16 shows that for the 0.9 m diameter PVC pipe, deformation increased at the top (50.40%) and right (54.06%) sections, while comparatively smaller increases were observed at the bottom (49.02%) and left (42.10%) sections, indicating varying stress redistribution within the EPS-based backfill.

The corresponding behaviour of flexible HDPE pipes is presented in Figures 17 and 18. For the 0.9 m diameter HDPE pipe (Figure 17), deformation generally increased with increasing backfill depth in all sections. Figure 18 shows a similar trend for the 1.2 m diameter HDPE pipe, although localized variations occurred due to differences in stress distribution. The increased deformation is primarily attributed to higher overburden pressure, differential soil settlement, reduced lateral support, and the reduced effectiveness of EPS-derived aggregates at greater burial depths. These results highlight the importance of optimizing backfill depth and EPS content to maintain the structural integrity and long-term performance of buried flexible pipes.

## 5. DISPLACEMENT CONTOURS

Pipe displacement was evaluated around the circumference at the crown (0°), spring-line (90°), invert (180°), and opposite spring-line (270°) to clearly represent deformation modes. Figures 19–21 illustrate the deformation behaviour of HDPE pipes buried at a depth of 0.9 m with sand containing 10–30% coarse EPS beads.

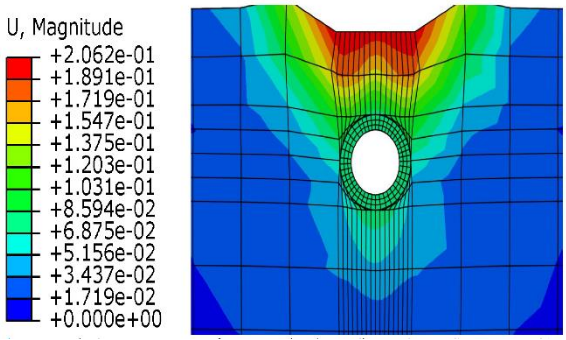


Figure. 19 Displacement contours for HDPE pipe (0.9m diameter) at EPS content =10% for depth of fill material = 0.9m.

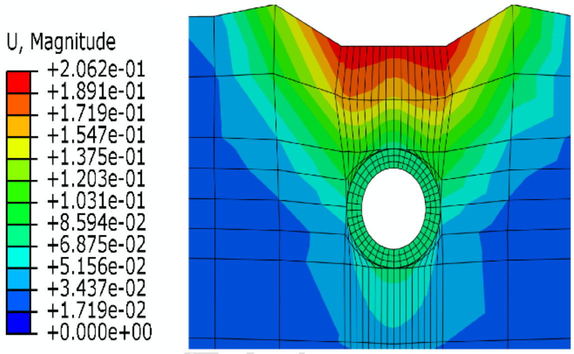


Figure. 20 Displacement contours for HDPE pipe (0.9m diameter) at EPS content = 20% for depth of fill material = 0.9m

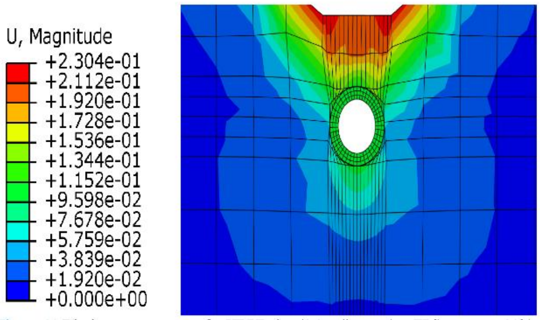


Figure. 21 Displacement contours for HDPE pipe (0.9m diameter) at EPS content = 30% for depth of fill material = 0.9m.

Figures 19–21 illustrate the deformation behaviour of HDPE pipes under loading and assess whether pipe displacement remains within permissible limits. The results show that, irrespective of the mixture composition, the deformation remained within acceptable limits for all percentages of coarse EPS beads. However, pipes containing 30% coarse EPS beads (Figure 20) exhibited better deformation resistance than those with 10% EPS beads (Figure 19), indicating an improved load-carrying capacity. The deformation patterns shown in Figures 19–21 are confined within a relatively small soil zone, confirming that the 0.9 m × 0.9 m trench dimensions are adequate for evaluating pipe response.

Although EPS beads are highly compressible, their proportion in the composite mixture was relatively small (0.05–0.20% for sand–EPS and 0.25–0.45% for sand–fly ash–cement–EPS mixtures). The addition of fly ash and cement increased the stiffness and bonding characteristics of the backfill, promoting controlled load redistribution while maintaining deformation within acceptable limits. Long-term settlement and creep behaviour of EPS-based composites were not considered and require further investigation.

## 5.1 Stress Distribution in Pipes

In addition to deformation, circumferential (hoop) stress and bending stress distributions were evaluated in the pipe wall. Maximum compressive stresses were observed near the crown, while tensile stresses developed near the spring lines due to ovalization. PVC pipes exhibited higher stress magnitudes due to greater stiffness compared to HDPE pipes. However, in all simulated cases, the computed stresses remained below allowable stress limits specified in relevant pipe design standards. These findings confirm that both deformation control and stress control criteria were satisfied for the investigated configurations.

# 6. CONCLUSION

The deformation behaviour of polyvinyl chloride and high-density polyethylene pipes buried in trenches filled with sand, sand-EPS derived aggregate, and sand-fly ash-cement-EPS derived aggregate is examined numerically in this research. The EPS beads that were used for modelling ranged in size from 4 to 5 mm. In sand-EPS derived aggregates, the content of EPS beads considered for modelling ranged from 0.05 to 0.20 %, whereas in sand-fly ash-cement-EPS produced aggregates, it varied from 0.25 to 0.45%. The pipes' diameter (0.5 to 1.2 m) and installation depth (0.3 to 0.9 m) were the additional variables considered for the modelling. The following findings are made considering the data and discussion from the earlier sections.

1. Enhancing the EPS derived aggregate in sand composite decrease the deformation of pipes but there are few cases where trend reverses such as at bottom and left side of the PVC pipe having diameter 0.9 m.
2. Enhancing the EPS derived aggregate in sand composite decrease the deformation of HDPE pipes having diameter 0.9 m and trend was reversed in HDPE pipe having diameter of 1.2 m at bottom and left side of the pipe.
3. Enhancing the fly ash in sand- EPS derived aggregate composite decrease the deformation of PVC pipes having diameter 0.5 m and trend was reversed in PVC pipe having diameter of 0.9 m.
4. Enhancing the fly ash in sand- EPS derived aggregate composite decrease the deformation of HDPE pipes having diameter 0.9 m at top, bottom and right side of pipe and slight increase in left side of pipe and trend continues in HDPE pipe having diameter of 1.2 m at top, bottom and left side of pipe and slight increase in right side of pipe.
5. Changing the diameter of pipe with respect to depth of backfill of sand-EPS derived composite decrease the deformation of PVC pipe (0.5 m diameter) at all sides of the pipe but trend was reversed in PVC (0.9 m diameter) pipe at top and right side of the pipe.
6. Changing the diameter of pipe with respect to depth of backfill of sand-EPS derived composite decrease the deformation of HDPE pipe (0.9 m diameter) at all sides of the pipe but trend was reversed in HDPE (1.2 m diameter) pipe at top and right side of the pipe.

**NOTATION**

EPS Expanded polystyrene

PVC Poly vinyl chloride

HDPE Hight density polythene

C Cohesion of the material

E Elastic Modulus of the Material

Dp Diameter of pipe

$K_O$ Lateral Earth Pressure Coefficient

$\phi$ Angle of friction

DT Depth of backfill

**ACKNOWLEDGMENT**

No artificial intelligence tools were used in the preparation of this manuscript.

**CONFLICT OF INTEREST**

The author declares that there are no conflicts of interest regarding individuals associated with the content presented in this paper.

**FUNDING DECLARATION**

This research received no specific grant from any funding agency**.**

**REFERENCES**

A . M. Partos and P . M. Kazaniwsky. (1987). Geoboard Reduces Lateral Earth Pressures . *Proc., Geosynthetics '87, Industrial Fabrics Association International*, 628–639. pp.

A. Kuliczkowski. (2001). *Rury kanalizacyjne. Własności materiałowe*. https://katalogi.uj.edu.pl/discovery/fulldisplay?docid=alma991005244569705067&context=L&vid=48OMNIS_UJA:uja&lang=pl&search_scope=MyInstitution&adaptor=Local%20Search%20Engine&tab=LibraryCatalog&query=sub,exact,Kanalizacja%20--%20budowa%20i%20konstrukcje,AND&mode=advanced&offset=0

Abdollahi, M., Tafreshi, S. N. M. and Leshchinsky, B. (2021). Protection of Buried Utilities against Repeated Loading: Application of Geogrid-EPS Geofoam System. *International Journal of Geomechanics*, *21*(9), 04021158. p. https://doi.org/10.1061/(ASCE)GM.1943-5622.0002120

Azizian, M., Tafreshi, S. N. M. and Darabi, N. J. (2020). Experimental evaluation of an expanded polystyrene (EPS) block-geogrid system to protect buried pipes. *Soil Dynamics and Earthquake Engineering*, *129*, 105965. p. https://doi.org/10.1016/J.SOILDYN.2019.105965

Bartlett, S. , N. D. , S. M. , and K. M. ,. (2000). *Use of Geofoam as Superlight weight Fill for I-15 Reconstruction*.

Castro, J. (2017). Groups of encased stone columns: Influence of column length and arrangement. *Geotextiles and Geomembranes*, *45*(2), 68–80. pp. https://doi.org/10.1016/J.GEOTEXMEM.2016.12.001

Chaallal, O., Arockiasamy, M. and Godat, A. (2014). Field Test Performance of Buried Flexible Pipes under Live Truck Loads. *Journal of Performance of Constructed Facilities*, *29*(5), 04014124. p. https://doi.org/10.1061/(ASCE)CF.1943-5509.0000624

Chen, B., Meng, Q., Yan, T., Wang, C. and Song, D. (2020). New Simplified Method for Analysis of Earth Pressure on the Imperfect Trench Installation Box Culvert. *International Journal of Geomechanics*, *20*(10), 04020193. p. https://doi.org/10.1061/(ASCE)GM.1943-5622.0001842

Edil, T. and Bosscher, P. (1994). Engineering Properties of Tire Chips and Soil Mixtures. *Geotechnical Testing Journal* , *17*(4), 453–464. pp. https://doi.org/10.1520/GTJ10306J

Hazarika, H. (2006). Stress–strain modeling of EPS geofoam for large-strain applications. *Geotextiles and Geomembranes*, *24*(2), 79–90. pp. https://doi.org/10.1016/J.GEOTEXMEM.2005.11.003

Horvath, J. S. (1998). *The Compressible-Inclusion Function of EPS Geofoam: An Overview of Concepts, Applications, and Products*. https://doi.org/10.13140/RG.2.2.21176.19207

Horvath, J. S. (2003). *Innovative Aspects of the Use of Expanded Polystyrene (EPS) on Boston's "Big Dig."* https://doi.org/10.13140/RG.2.2.14884.73605

Kang, J., Im, H. and Park, J. S. (2020). The effect of load reduction on underground concrete arch structures in embedded trench installations. *Tunnelling and Underground Space Technology*, *98*, 103240. p. https://doi.org/10.1016/J.TUST.2019.103240

Khajeh, A., Jamshidi Chenari, R. and Payan, M. (2020). A Review of the Studies on Soil-EPS Composites: Beads and Blocks. *Geotechnical and Geological Engineering 2020 38:4*, *38*(4), 3363–3383. pp. https://doi.org/10.1007/S10706-020-01252-2

Khalaj, O., Azizian, M., Darabi, N. J., Tafreshi, S. N. M. and Jirková, H. (2020). The Role of Expanded Polystyrene and Geocell in Enhancing the Behavior of Buried HDPE Pipes under Trench Loading Using Numerical Analyses. *Geosciences 2020, Vol. 10, Page 251*, *10*(7), 251. p. https://doi.org/10.3390/GEOSCIENCES10070251

Khalaj, O., Siabil, S. M. A. G., Azizian, M., Tafreshi, S. N. M., Masek, B., Kepka, M., Kavalir, T., Krizek, M., Jirkova, H., Khalaj, O., Siabil, S. M. A. G., Azizian, M., Tafreshi, S. N. M., Masek, B., Kepka, M., Kavalir, T., Krizek, M. and Jirkova, H. (2020). Geomechanics and Engineering. *Geomechanics and Engineering*, *22*(6), 475. p. https://doi.org/10.12989/GAE.2020.22.6.475

Khan, M. I. and Meguid, M. A. (2021). Evaluating the Role of Geofoam Properties in Reducing Lateral Loads on Retaining Walls: A Numerical Study. *Sustainability 2021, Vol. 13, Page 4754*, *13*(9), 4754. p. https://doi.org/10.3390/SU13094754

Kim, K. and Yoo, C. H. (2005). Design Loading on Deeply Buried Box Culverts. *Journal of Geotechnical and Geoenvironmental Engineering*, *131*(1), 20–27. pp. https://doi.org/10.1061/(ASCE)1090-0241(2005)131:1(20)

Kliszczewicz, B. and Kowalska, M. (2020). Numerical Study of the Use of Tyre-Derived-Aggregate (TDA) as the Backfill Above Flexible PVC Pipeline. *IOP Conference Series: Materials Science and Engineering*, *960*(3), 032044. p. https://doi.org/10.1088/1757-899X/960/3/032044

Kumar, M., Pratap, B., Azhar, M., Mondal, S. and Singh, R. P. (2025). The Utilization of Plastic Waste for Stabilizing Expansive Soil Subgrade: A Critical Review. *Civil Engineering Infrastructures Journal*, *58*(2), 203–229. pp. https://doi.org/10.22059/CEIJ.2024.369358.1991

Lee, S. J., Lee, S. R. and Kim, Y. S. (2003). An approach to estimate unsaturated shear strength using artificial neural network and hyperbolic formulation. *Computers and Geotechnics*, *30*(6), 489–503. pp. https://doi.org/10.1016/S0266-352X(03)00058-2

Onyelowe, K. C., Gnananandarao, T. and Ebid, A. M. (2022). Estimation of the erodibility of treated unsaturated lateritic soil using support vector machine-polynomial and -radial basis function and random forest regression techniques. *Cleaner Materials*, *3*. https://doi.org/10.1016/J.CLEMA.2021.100039/REFERENCES

Onyelowe, K. C., Gnananandarao, T. and Nwa-David, C. (2021). Sensitivity analysis and prediction of erodibility of treated unsaturated soil modified with nanostructured fines of quarry dust using novel artificial neural network. *Nanotechnology for Environmental Engineering*, *6*(2), 37. p. https://doi.org/10.1007/s41204-021-00131-2

Santos, R. R. V., Kang, J. and Park, J. S. (2020). Effects of embedded trench installations using expanded polystyrene geofoam applied to buried corrugated steel arch structures. *Tunnelling and Underground Space Technology*, *98*, 103323. p. https://doi.org/10.1016/J.TUST.2020.103323

Schmidt, B. (2011). Earth Pressures at Rest Related to Stress History. *Https://Doi.Org/10.1139/T66-028*, *3*(4), 239–242. pp. https://doi.org/10.1139/T66-028

Shahu, J. T. and Reddy, Y. R. (2011). Clayey Soil Reinforced with Stone Column Group: Model Tests and Analyses. *Journal of Geotechnical and Geoenvironmental Engineering*, *137*(12), 1265–1274. pp. https://doi.org/10.1061/(ASCE)GT.1943-5606.0000552

Spangler, M. G. (n.d.). *A Practical Application of the Imperfect Ditch Method of Construction*.

Spangler, M. G. (1950). *FIELD MEASUREMENTS OF THE SETTLEMENT RATIOS OF VARIOUS HIGHWAY CULVERTS*.

Talal Awwad; Salma Al Kodsi. (2018). *A Comparison of Numerical Simulation Models to Determine the Location of Neutral Plane | ISSMGE*. 19th International Conference on Soil Mechanics and Geotechnical Engineering (Seoul). https://www.issmge.org/publications/publication/a-comparison-of-numerical-simulation-models-to-determine-the-location-of-neutral-plane

Tammineni Gnananandarao, Rakesh Kumar Dutta, V. N. K. and M. S. K. (2022). Soft Computing Based Prediction of Unconfined Compressive Strength of Fly Ash Stabilised Organic Clay. *Journal of Soft Computing in Civil Engineering*.

Vaslestad, J. , J. T. H. , and H. W. ,. (1994). TransportationResearch Record. 1415. *Transportation Research Board, Wash-Ington, D.C.*, 58–68. pp.

Vaslestad, J., Johansen, H. and Holm, W. (n.d.). *Load Reduction on Rigid Culverts Beneath High Fills: Long-Term Behavior*.

Yaghoobzadeh, S., Azizkandi, A. S., Salehzadeh, H. and Hasanaklou, S. H. (2021). Effect of EPS Beads on the Behavior of Sand–EPS and Slope Stability Using Triaxial and Centrifuge Tests. *International Journal of Civil Engineering*, *19*(11), 1269–1282. pp. https://doi.org/10.1007/S40999-021-00617-9/TABLES/13

Zhu, L., Wen, K., Tong, R. and Li, M. (2022). Dynamic Shear Strength Characteristics of Lightweight Sand-EPS Soil. *Sustainability 2022, Vol. 14, Page 7397*, *14*(12), 7397. p. https://doi.org/10.3390/SU14127397